Observing and modeling wideband generation of non-linear interference

# Observing and Modeling the Wideband Generation of Non-Linear Interference

**Emanuele Virgillito, Andrea D'Amico, Alessio Ferrari, Vittorio Curri**

*DET, Politecnico di Torino, Torino, Italy*

*emanuele.virgillito@polito.it*

**Abstract:** Optical line systems are going beyond the C-band by exploiting multi-band transmission to expand the fiber capacity without installing new fiber cables. Moreover, operators are progressively pushing towards the implementation of the open optical network paradigm. This requires the capability to quickly estimate the lightpath Quality-of-Transmission (QoT) given by the generalized signal-to-noise ratio (GSNR), including both the effects of ASE noise and non-linear interference (NLI) accumulation. In order to predict the effect of NLI on GSNR degradation of multi-band OLS, we first observe that the NLI generation can be spectrally disaggregated, by separating the single-channel – self-phase modulation (SPM) – from the multi-channel effects – cross-phase modulation (XPM). Then, relying on the Gaussian-Noise model hypotheses, we derive a mathematical model to assess the multi-channel impairments, validated by accurate split-step simulations. We show that the model conservatively predicts the disaggregated multi-channel NLI intensity with excellent accuracy.

## 1. Introduction

To afford the predicted growth in data traffic over the next years [1], operators require more capacity from the installed infrastructure [2] that is approaching saturation of the C-band fast. To this aim, multi-band line-systems have been developed and already installed to enlarge the capacity per fiber. Moreover, the disaggregated optical networks implementing the openness paradigm within a SDN environment, starting from the *open* optical line systems (OLS), is a common request of the operators. In managing the network down to the physical layer, the SDN controller needs a full and reliable abstraction of the OLSs, which is represented by the degradation of the generalized SNR, $\mathrm{GSNR} = (\mathrm{OSNR}^{-1} + \mathrm{SNR_{NL}}^{-1})^{-1}$. The GSNR has to take into account both the intensity of the ASE noise through the OSNR and of the NLI disturbance through the non-linear SNR, namely the $\mathrm{SNR_{NL}}$ [3]. Several analytic models have been developed for NLI evaluation with excellent accuracy up to the C-band, but a clear assessment on the multi-band generation of NLI has not been yet proposed. In [4, 5] the NLI expression has been derived approaching the non-linear Schrodinger equation (NLSE) in the frequency domain and abstracting the non-linear interaction as a frequency-distributed Four-Wave Mixing (FWM) among the Gaussian noise components. In particular, the Gaussian noise (GN) model [4, 6] belongs to this family as it estimates the NLI power as an additive Gaussian noise. The GN model has been recently generalized by including frequency and space variations of gains and losses [7], but still keeping a spectrally-aggregated approach. The GN model has proven an excellent capability in predicting the $\mathrm{SNR_{NL}}$ and has been exploited within several QoT-E, and tested in multi-vendor scenarios up to 3 THz of occupied bandwidth [8]. In [9–12] the NLSE inter-channel and each intra-channel NLI contribution is treated separately. The problem has been approached in time domain observing the collision among pulses. [13] proposes the enhanced GN (EGN) model by correcting the GN model and reaching an excellent accuracy, but with quite large computational time.

In this work, we approach the NLI generation disaggregating the single-channel – self-phase modulation (SPM) – and the multi-channel effects – cross-phase modulation (XPM) –, in order to isolate the multi-band phenomenon. Then, we apply the Gaussian-noise hypotheses and derive an analytic expression leading to the power spectral density (PSD) of the NLI component generated by each side-channel, with respect the channel under test (CuT). We finally verify the XPM model against split-step Fourier method (SSFM) simulations, showing a remarkable accuracy in the fast prediction of the overall $\mathrm{SNR_{NL}}$ with a computational-time of some tens of seconds.

## 2. Observing and modelling the disaggregated NLI generation

In this work, we test and exploit the *disaggregation hypothesis* of non-linear effects, according to which the overall $\mathrm{P_{NLI}}$ can be *disaggregated* as the sum of the SPM, XPM and FWM contributions. Given the characterizing features of the fiber and the channels that we analyze, the FWM term is negligible [12]. Therefore, on the CuT, we obtain the following expressions of the $\mathrm{P_{NLI}}$ and the $\mathrm{SNR_{NL}}$, respectively:

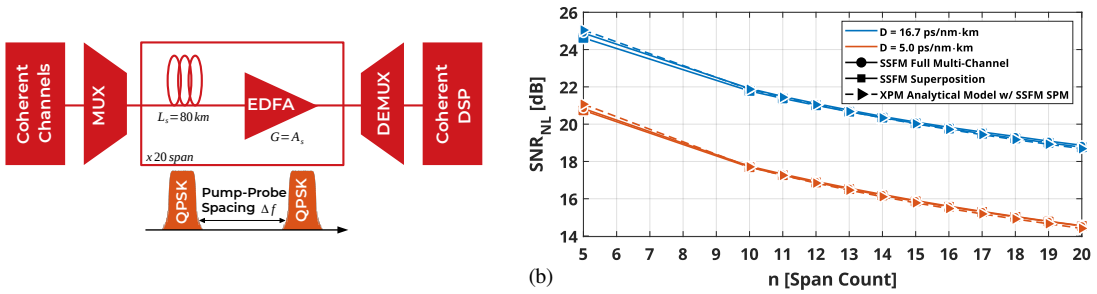


Fig. 1: (a) The simulation layout. (b) Central channel $\mathrm{SNR_{NL}}$ of a 21 channels DWDM comb along a 20x80 km spans transmission line with 0 dBm of channel power. Results have been obtained with full 21 multi-channel simulation (circles), effects superposition by single-channel simulations for SPM and PP simulations for XPM (squares), analytic model estimations with simulated SPM noise (triangles).

$$\mathrm{P_{NLI}} = \mathrm{P_{NLI,0}} + \sum_{k\neq 0} \mathrm{P_{NLI,}}k \quad \Rightarrow \quad \mathrm{SNR_{NL}^{-1}} = \mathrm{SNR_{NL,0}}^{-1} + \sum_{k\neq 0} \mathrm{SNR_{NL,}}k^{-1}\,, \tag{1}$$

where the subscripts 0 and $k$ indicate the SPM term and the XPM term generated, in turn, by the $k$ labelled channel, respectively. To test the validity of the disaggregation hypothesis, we have performed SSMF simulations of a 21-channel transmission scenarios. The CuT has been set to the central channel of the comb and its $\mathrm{SNR_{NL}}$ has been measured as a QoT figure of merit in three different conditions: the full multi-channel configuration, which quantifies the left-hand terms in Eq. 1; the single-channel propagation, which assesses the SPM contribution; the pump ($k$ channel) and probe (CuT) configurations (PP), separately for each $k$, that quantify the terms $\mathrm{SNR_{NL,}}k$. The transmission line is made of 20 identical spans of 80 km length as sketched in Fig.1(a), operated in transparency conditions by ideal amplifiers without any ASE noise to isolate the $\mathrm{SNR_{NL}}$. The fiber loss and non-linear coefficients are set to $\alpha_{dB} = 0.18$ dB/km and $\gamma = 1.27\ (\mathrm{W\cdot km})^{-1}$. To assess the scaling with fiber dispersion, we have considered both $D = 16.7\ \mathrm{ps/(nm\cdot km)}$ and $D = 5\ \mathrm{ps/(nm\cdot km)}$. All the channels are $R_s = 32$ GBaud, PM-QPSK modulated channels on the $\Delta f = 50$ GHz grid. In the PP configuration, the probe power has been kept low at -20 dBm, to avoid the SPM contribution and isolate the XPM-generated NLI. Through the whole analysis, we address with $k$ the channel whose spacing from the CuT is $k\Delta f$ GHz. We have then compared the $\mathrm{SNR_{NL}}$ along the optical spans obtained with full multi-channel simulation to the $\mathrm{SNR_{NL}}$ obtained by aggregating the single-channel and PP SSFM results as in Eq.1. As shown in Fig.1(b) by the circles and square curves, the disaggregated approach is accurate: the SPM and XPM superposition overlaps with the overall multi-channel $\mathrm{SNR_{NL}}$ values at each number of spans observed for both the fiber types. This implies that it is meaningful to address separately the analytic description of the SPM and XPM NLI generation. We focus on the latter.

The disaggregation hypothesis enables to analyze the XPM as a PP configuration with variable $k$. In the considered typical scenario, the pump walk-off with respect to the probe exceeds a symbol period after one span, thus the XPM terms of two cascaded spans are statistical independent from each other. Therefore, the NLI contributions of each span add-up independently:

$$\mathrm{P_{NLI,}}k = \sum_{n}^{N_s} \mathrm{P_{NLI,}}k,n = N_s \int_{\Omega_s}, \frac{\mathrm{d}\omega}{2\pi}\, \mathscr{G}_k(\omega) \tag{2}$$

where $N_s$ is the number of spans and $\Omega_s = R_s/2\pi$ and $\mathscr{G}_k(\omega)$ is the PSD of the NLI generated by the $k$-th pump along each span. In the last step of Eq.2, we suppose that the incoming fields have the same statistical features at each span (together with the identical spans condition). In particular, we assume the input signals to be a Gaussian stochastic processes for each span:

$$E(z=0,t) = E_0(z=0,t) + E_k(z=0,t) = \sum_{l_0=-\infty}^{\infty} \rho_{l_0} s_0(t - l_0 T_s) + \sum_{l_k=-\infty}^{\infty} \rho_{l_k} s_k(t - l_k T_s)\,, \tag{3}$$

where $\rho_{l_0,k}$ are two statistically independent Gaussian processes whose variances are equal to the channels powers. $s_{0,k}$ define the signal waveforms that, in the frequency domain, have support on the probe and the pump bandwidths, respectively. In the perspective of QoT estimation for planning purposes, the Gaussian assumption does not reduce the generality of this derivation, since this condition is the worst-case as widely shown in the literature. The NLI PSD for a single span can be then calculated addressing the first order non-linear solution of the Manakov equation [14] in the PMD scenario:

$$\partial_z \hat{N}_{0;x,y}(z,\omega) = -i\gamma\left(\frac{8}{9}\right) e^{-2\alpha z} \iint_{-\infty}^{\infty} \frac{\mathrm{d}\omega_1}{2\pi}\frac{\mathrm{d}\omega_2}{2\pi}\, e^{-\frac{i}{2}\beta_2\left[\omega_1^2-(\omega_1-\omega_2)^2+(\omega-\omega_2)^2-\omega^2\right]z} \times$$
$$\times\left\{\left[\hat{E}_k(\omega_1)\cdot\hat{E}_k^*(\omega_1-\omega_2)\right]\hat{E}_{0;x,y}(\omega-\omega_2)+\left[\hat{E}_0(\omega_1)\cdot\hat{E}_k^*(\omega_1-\omega_2)\right]\hat{E}_{k;x,y}(\omega-\omega_2)\right\} \quad (4)$$

where $\cdot$ stands for the standard scalar product in the polarization space. By supposing that the channels distributions remain constant trough the whole span length, we obtain the following expression of the XPM noise PSD:

$$\begin{aligned}
\mathscr{G}_k(\omega) &= \mathscr{F}^{-1}\left[\langle N^*(z,t)\cdot N(z,t+\tau)\rangle\right] = \\
&= 2\gamma^2\left(\frac{8}{9}\right)^2\left\{\left[2\left(\left\langle|\rho_{x,k}|^4\right\rangle-\left\langle|\rho_{x,k}|^2\right\rangle^2\right)+\left(\left\langle|\rho_{y,k}|^4\right\rangle-\left\langle|\rho_{y,k}|^2\right\rangle^2\right)\right]\left\langle|\rho_{x,0}|^2\right\rangle+\right. \\
&\quad \left.+\left\langle|\rho_{y,0}|^2\right\rangle\left\langle|\rho_{y,k}|^2\right\rangle\left\langle|\rho_{y,k}|^2\right\rangle\right\}\left(\frac{2\pi}{\Omega_s}\right)^3\iint_{-\infty}^{\infty}\frac{\mathrm{d}\omega_1}{2\pi}\frac{\mathrm{d}\omega_2}{2\pi}\, I_k(\omega_1)I_k(\omega_1-\omega_2)I_0(\omega-\omega_2)L^2(\omega;\omega_1,\omega_2) = \\
&= \frac{4\pi\gamma^2}{\Omega_s^3}\frac{64}{81}\left\{2P_{k,x}^2P_{0,x}+P_{k,y}^2P_{0,x}+P_{0,x}P_{k,y}P_{k,x}\right\}\iint_{-\infty}^{\infty}\mathrm{d}\omega_1\mathrm{d}\omega_2\, I_k(\omega_1)I_k(\omega_1-\omega_2)I_0(\omega-\omega_2)L^2(\omega;\omega_1,\omega_2) \quad (5)
\end{aligned}$$

In Eq.5, the operator $\langle\cdots\rangle$ stands for the expectation value over the realizations of a stochastic process. $I_{0,k}$ are, in turn, the characteristic functions of the probe and pump bandwidths, whereas:

$$L^2(\omega;\omega_1,\omega_2) = \left|\int_0^L \mathrm{d}z\, e^{-2\alpha z}e^{-\frac{i}{2}\beta_2\left[\omega_1^2-(\omega_1-\omega_2)^2+(\omega-\omega_2)^2-\omega^2\right]z}\right|^2 \quad (6)$$

In particular, $|L|$ equals the effective length when $\beta_2 = 0$.

## 3. Validation and Results

In section 2 we have shown that the overall $\mathrm{P_{NLI}}$ can be *disaggregated* as the sum of SPM and XPM pumps contributions. Here, we validate the approach focusing on the NLI generated by a single pump, thus by comparing the results of PP simulations with the outcomes of the analytic model of Eq.5. We first look at the accumulation of the XPM along the fiber link. Since the $\mathrm{P_{NLI}}$ adds up along the spans as in Eq.2, the $\mathrm{SNR_{NL},}_k$ can be obtained as:

$$\mathrm{SNR_{NL},}_k{}^{-1} = \sum_{n=1}^{N_s}\mathrm{SNR_{NL},}_{k,n}{}^{-1} \quad (7)$$

being $\mathrm{SNR_{NL},}_{k,n}$ the SNR degradation due to the XPM noise introduced by the $n$-th span. Fig.2(a,b) show the accumulation along the fiber link of the XPM noise generated by the $k = 4$ pump by looking at the $\mathrm{SNR_{NL},}_k$ at the output of each fiber span measured by SSMF together with the model prediction. The corresponding SNR degradation due to the single spans $\mathrm{SNR_{NL},}_{k,n}$ is instead reported in Fig.2(c,d). Here, the pump power is set to 3 dBm to ensure that the amount of NLI is measurable with respect to the back to back performance already after 1 or 2 spans of propagation. The model curves assume the worst-case Gaussian-distributed symbols. This is practically verified in deployed systems due to the effect of fiber dispersion after a few spans. Hence, to assess the convergence of the SSMF observations to the model, we perform simulations by progressively pre-applying dispersion to the signal. We investigate from no predistortion up to an equivalent pre-propagation of 6 spans (from 0 ps/nm up to 8016 ps/nm and 2400 ps/nm for $D = 16.7$ ps/(nm $\cdot$ km) and $D = 5$ ps/(nm $\cdot$ km), respectively). The $\mathrm{SNR_{NL},}_{k,n}$ curves of Fig.2(c,d) show that, for both fiber dispersion values, about 6 spans of accumulated dispersion are enough to reach the Gaussian assumption so that the amount of XPM NLI converges to the value predicted by the model. The convergence to a constant $\mathrm{SNR_{NL}}$ degradation at each span proves also, as evident in Fig.2(a,b), that the $\mathrm{P_{NLI},}_k$ grows linearly with the fiber spans as predicted by the model. Furthermore, the analytic model always returns a conservative $\mathrm{SNR_{NL}}$ value. The gap between the model prediction and the $\mathrm{SNR_{NL}}$ of the non-distorted scenario, after 20 span of propagation, is 1.17 dB and 1.01 dB, for $D = 16.7$ ps/(nm $\cdot$ km) and $D = 5$ ps/(nm $\cdot$ km), respectively. In Fig.3, we show the scaling of the $\mathrm{SNR_{NL},}_k$ with the bandwidth by comparing the $\mathrm{SNR_{NL},}_k$ obtained from SSFM simulations and model, varying the spacing and fiber dispersion. The analytic estimation matches very well the SSFM results with 10 spans of predistortion. From 10 to 20 span a 3 dB degradation can be observed, as expected. Also, the nearly 1 dB gap between the model and the non distorted case is confirmed for each frequency spacing at 20 spans. This gap widens instead at larger spacing and 10 spans due to simulation inaccuracies. Finally, we test the analytic model to predict the QoT of the multi-channel scenario and test the superposition principle in Fig.1(b). The total $\mathrm{SNR_{NL}}$ is evaluated as in Eq.1. The SPM term $\mathrm{P_{NLI,0}}$ has been obtained by means of SSFM simulation, while the XPM contributions of the 20 pumps has been estimated with the analytic model. The resulting $\mathrm{SNR_{NL}}$ curves along the line for dispersions of $D = 16.7$ ps/(nm $\cdot$ km) and $D = 5$ ps/(nm $\cdot$ km) are reported as triangles in Fig.1(b). The curves show overwhelmingly accurate results that overlap with the full multi-channel SSMF simulations.

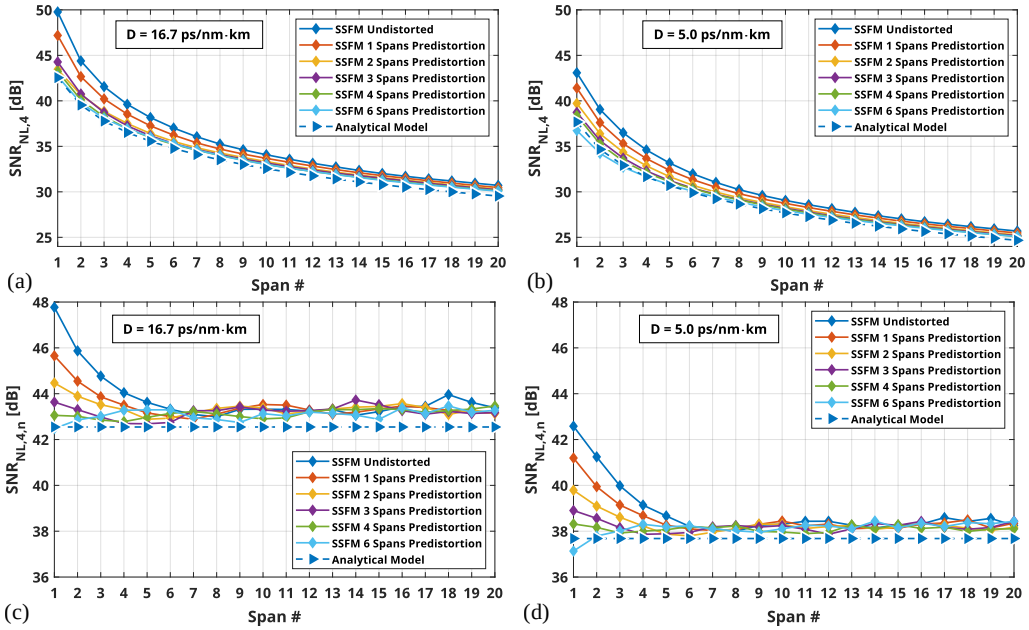


Fig. 2: $\mathrm{SNR_{NL}}$ accumulation along the fiber spans simulated by SSMF with applied predistortion of 0 to 6 spans and estimated by the analytic model for (a) $D = 16.7$ ps$/$(nm$\cdot$km), (b) $D = 5$ ps$/$(nm$\cdot$km). Corresponding $\mathrm{SNR_{NL}}$ degradation introduced by each span for (c) $D = 16.7$ ps$/$(nm$\cdot$km), (d) $D = 5$ ps$/$(nm$\cdot$km)

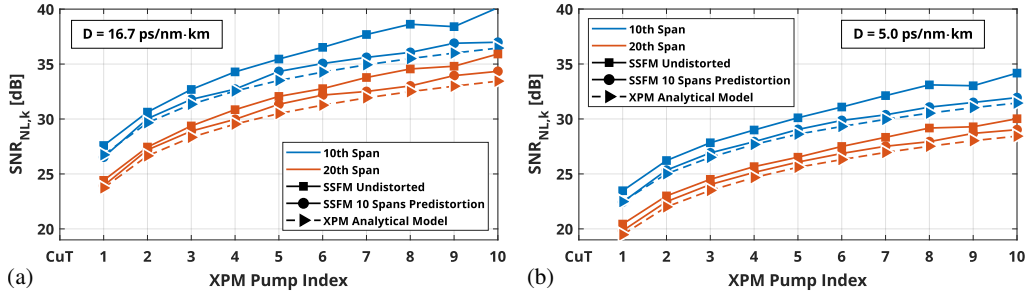


Fig. 3: $\mathrm{SNR_{NL}}$ on the CuT originated by a single XPM pump simulated with (squares) and without (circles) predistortion and estimated by the analytic model (triangles) after 10 (blue) and 20 (red) span and for (a) $D = 16.7$ ps$/$(nm$\cdot$km), (b) $D = 5$ ps$/$(nm$\cdot$km).

## 4. Conclusions

Starting from the existing and well established models, we have present a renewed, disaggregated, analytic model aiming at a finer estimation of the multi-channel NLI generation. We first proved the disaggregation hypothesis, then we tested the model and show that it gives an accurate prediction of the wideband NLI generation requiring a computational time of the order of tens of seconds only.

## 5. Acknowledgement

The work has been supported by Telecom Infra Project within the OOPT-Raman activities.

## References

[1] Cisco, tech. rep., Cisco Visual Networking Index: Forecast and Methodology, 2017-2022, 2018.
[2] G. Wellbrock et al., *ECOC*, IEEE, 2014, pp. 1–3.
[3] V. Curri et al., *J. of Lightwave Tech.* 33.18 (2015), pp. 3921–3932.
[4] A. Carena et al., *J. of Lightwave Tech.* 30.10 (2012), pp. 1524–1539.
[5] P. Johannisson et al., *J. of Lightwave Tech.* 31.8 (2013), pp. 1273–1282.
[6] V. Curri et al., *Optics express* 21.3 (2013), pp. 3308–3317.
[7] M. Cantono et al., *IEEE / OSA JLT* 36.15 (2018), pp. 3131–3141.
[8] M. Filer et al., *J. of Lightwave Tech.* 36.15 (2018), pp. 3073–3082.
[9] A. Bononi et al., *Optics Express* 20.7 (2012), p. 7777.
[10] A. Mecozzi et al., *J. of Lightwave Tech.* 30.12 (2012), pp. 2011–2024.
[11] M. Secondini et al., *Photonics Technology Letters* 24.22 (2012), pp. 2016–2019.
[12] R. Dar et al., *J. of Lightwave Tech.* 34.2 (2016), pp. 593–607.
[13] A. Carena et al., *Optics express* 22.13 (2014), pp. 16335–16362.
[14] M. Cantono et al., *OFC Conference*, OSA, 2018, W1G.4.